Journal of Atmospheric and Solar-Terrestrial Physics 138-139 (2016) 93–105

Contents lists available at ScienceDirect

Journal of Atmospheric and Solar-Terrestrial Physics

journal homepage: www.elsevier.com/locate/jastp

Research paper

Effects of the intense geomagnetic storm of September–October 2012 on the equatorial, low- and mid-latitude F region in the American and African sector during the unusual 24th solar cycle

R. de Jesus [a,d,*], P.R. Fagundes [a], A. Coster [b], O.S. Bolaji [c], J.H.A. Sobral [d], I.S. Batista [d], A.J. de Abreu [a,e], K. Venkatesh [a], M. Gende [f], J.R. Abalde [a], S.G. Sumod [g]

[a] Universidade do Vale do Paraíba /IP & D, São José dos Campos, SP, Brazil
[b] Haystack Observatory, Massachusetts Institute of Technology (MIT), Westford, Massachusetts, USA
[c] Department of Physics, University of Lagos, Akoka, Lagos, Nigeria
[d] Instituto Nacional de Pesquisas Espaciais (INPE), São José dos Campos, SP, Brazil
[e] Instituto Tecnológico de Aeronáutica (ITA), Divisão de Ciências Fundamentais, São José dos Campos, SP, Brazil
[f] Facultad de Ciencias Astronómicas y Geofísicas, Universidad Nacional de La Plata, La Plata, Argentina
[g] S.H College Thevara, Kochi-13, Mahatma Gandhi University, India

ARTICLE INFO

Article history:
Received 8 May 2015
Received in revised form
7 December 2015
Accepted 29 December 2015
Available online 30 December 2015

Keywords:
Space weather
Geomagnetic storm
Ionosphere
Ionospheric irregularities

ABSTRACT

The main purpose of this paper is to investigate the response of the ionospheric F layer in the American and African sectors during the intense geomagnetic storm which occurred on 30 September–01 October 2012. In this work, we used observations from a chain of 20 GPS stations in the equatorial, low- and mid-latitude regions in the American and African sectors. Also, in this study ionospheric sounding data obtained during 29th September to 2nd October, 2012 at Jicamarca (JIC), Peru, São Luis (SL), Fortaleza (FZ), Brazil, and Port Stanley (PST), are presented. On the night of 30 September–01 October, in the main and recovery phase, the h´F variations showed an unusual uplifting of the F region at equatorial (JIC, SL and FZ) and mid- (PST) latitude stations related with the propagations of traveling ionospheric disturbances (TIDs) generated by Joule heating at auroral regions. On 30 September, the VTEC variations and foF2 observations at mid-latitude stations (American sector) showed a long-duration positive ionospheric storm (over 6 h of enhancement) associated with large-scale wind circulations and equatorward neutral winds. Also, on 01 October, a long-duration positive ionospheric storm was observed at equatorial, low- and mid- latitude stations in the African sector, related with the large-scale wind circulations and equatorward neutral winds. On 01 and 02 October, positive ionospheric storms were observed at equatorial, low- and mid-latitude stations in the American sector, possibly associated with the TIDs and an equatorward neutral wind. Also, on 01 October negative ionospheric storms were observed at equatorial, low- and mid-latitude regions in the American sector, probably associated with the changes in the O/N_2 ratio. On the night of 30 September–01 October, ionospheric plasma bubbles were observed at equatorial, low- and mid- latitude stations in the South American sector, possibly associated with the occurrence of geomagnetic storm.

1. Introduction

A geomagnetic storm is the result of the energy transfer from the solar wind to the magnetosphere (Gonzalez and Tsurutani, 1987; Tsurutani et al., 1997). There is a strong relationship between the occurrence of geomagnetic storms and ionospheric disturbances. The responses of ionosphere–thermosphere system in the mid-latitude region during geomagnetic storms have been extensively documented, during solar cycles 21, 22 and 23 (e.g., Prolss and Jung, 1978; Yeh et al., 1991; Pavlov, 1994; Richards and Wilkinson, 1998; Foster and Rich, 1998; Huang et al., 2003; Keskinen et al., 2004; Foster and Rideout, 2005; Basu et al., 2005; Annakuliev et al., 2005; Foster et al., 2007; Basu et al., 2008; Borries et al., 2009; Heelis et al., 2009 and references therein). Other investigators have studied the ionospheric response of equatorial and low- latitude F region during geomagnetic storms in solar cycles 21, 22 and 23 (e. g., Batista et al., 1991; Fejer and Scherliess, 1997; Abdu, 1997; Sobral et al., 1997; Abdu et al., 1998; Reddy and Mayr, 1998; Sobral et al., 2001; Batista et al., 2006; de

* Correspondence to: Av. Shishima Hifumi, 2911, Urbanova, 12244-000 São José dos Campos, SP, Brazil.
E-mail address: jesus.rodolfo@hotmail.com (R. de Jesus).

http://dx.doi.org/10.1016/j.jastp.2015.12.015
1364-6826/

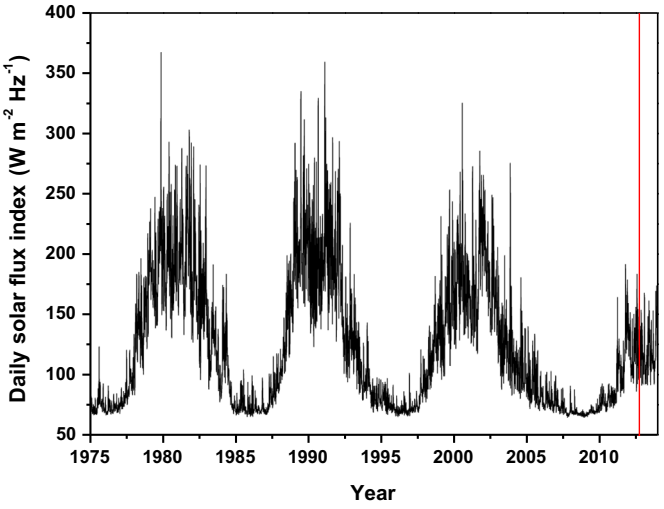

Fig. 1. The 10.7 cm solar flux index variations during 1975–2013. The vertical red line represents the days of September 30 and October 1, 2012 (period in which an intense geomagnetic storm occurred). (For interpretation of the references to color in this figure, the reader is referred to the web version of this article.)

Abreu et al., 2010a; Sahai et al., 2011; Klimenko et al., 2011; Batista et al., 2012; de Jesus et al. 2012). However, the morphology of the equatorial, low- and mid- latitude due to the intense geomagnetic storms have not been well covered during solar cycle 24, particularly in the American and African sectors. The effects of the intense geomagnetic storms on the equatorial, low- and mid- latitude ionosphere are important space weather issues. The interest in these investigations is associated with the current lack of understanding and our inability to predict the response of the upper atmosphere due to geomagnetic storms.

It should be mentioned that the solar cycle 24 shows entirely distinct characteristics as compared to earlier solar cycles (see Fig. 1). The solar activity levels can be represented by the decimetric solar flux index expressed in F10.7 flux units ($Wm^{-2}\,Hz^{-1}$). Fig. 1 shows the F10.7 variations from January 1975 to December 2013. The vertical red line in Fig. 1 represents the days 30 September and 1 October 2012 (geomagnetic disturbed period investigated). Fig. 1 shows that in solar cycle 24 the period of low solar activity was longer than those in other solar cycles. Fig. 1 also shows clearly that the values of F 10.7 are smaller in solar cycle 24 than those in previous solar cycles, especially during the period of high solar activity. The maximum values of F10.7 in solar cycle 21, 22 and 23 are 367, 359.2 and 325.1, respectively. The 191.6 was the maximum (value of F10.7) in cycle 24 up through 2012. The geomagnetic storm analyzed in this investigation occurred during the period of high solar activity in solar cycle 24, with the F10.7 flux values ranging from 128 to 136.

During the recent past, several investigators (e.g., Danilov and Morozova, 1985; Schunk and Sojka, 1996; Abdu, 1997; Buonsanto, 1999; Danilov, 2013) have reviewed the effects of geomagnetic storms at low-, mid- and high- latitude regions. During the periods of intense geomagnetic disturbances, a large amount of energy is dissipated in the polar region, which leads to profound changes in the global winds circulation via Joule heating (Schunk and Sojka, 1996). According to Buonsanto (1999), if the heating imposed over the high latitudes due to the solar wind via the magnetosphere are impulsive, the equatorward winds will take the form of equatorward surges or traveling atmospheric disturbances (TADs). It should be mentioned that TADs can manifest themselves in the ionosphere as traveling ionospheric disturbances (TIDs) (Hunsucker, 1982; Hocke and Schlegel, 1996; Buonsanto, 1999).

Geomagnetic disturbances could initiate positive ionospheric storms (positive phase), which is characterized by the electron density greater than normal (average of the quiet days) values (Prolss, 1993; Buonsanto, 1999; Sahai et al., 2005; de Abreu et al., 2010a, 2011). Also, the geomagnetic storms could initiate negative ionospheric storm (negative phase). This case is when the electron density value is significantly reduced compared to the normal pre-event value when no stormy condition is in place (quiet period) (Schunk and Sojka, 1996; Mansilla and Zossi, 2012). It is generally accepted that the negative ionospheric storms are due to composition (O/N_2 density ratio) changes (Prolss, 1980; Buonsanto, 1999; Sahai et al., 2009a, 2009b). However, for the positive ionospheric storms different mechanisms are proposed. Prolss (1995) has pointed out that positive ionospheric storms are due to an enhancement in the equatorward neutral winds arising from the auroral latitude energy injection.

In this paper, we carried out investigations to understand the response of the equatorial, low- and mid- latitude ionospheric F region in the American and African sectors during the intense geomagnetic storm which occurred between 30 September and 01 October 2012 (a period of high solar activity during the unusual 24th solar cycle). We used observations from 20 GPS stations and 4 digital ionosonde stations. The prime objectives of the present study are to investigate the generation or suppression of the equatorial ionospheric irregularities and dynamics of the ionosphere in the American and African sectors during this intense geomagnetic storm.

2. Observations

In this study, we present and discuss the simultaneous ionospheric sounding observations (minimum F-region virtual height, h′F, and F-region critical frequency, foF2) from Jicamarca (every 30 min; equatorial station and hereafter referred as JIC), Peru, São Luis (every 10 min; equatorial station and hereafter referred as SL), Fortaleza (every 10 min; a near equatorial station and hereafter referred as FZ), Brazil, and Port Stanley (every 30 min; a mid-latitude station and hereafter referred as PST), during the period from 29 September to 02 October 2012. Also, vertical total electron content (VTEC) from 20 Global Positioning System (GPS) receivers in the American and African sectors (see Table 1 and Fig. 2), during the period from 29 September–02 October 2012, are presented. The GPS observations are also used to obtain the phase fluctuations (rate of change of TEC) and measurements of scintillations (S4, amplitude scintillation index). It should be mentioned that the VTEC is calculated in units of TEC (1 TEC unit $=10^{16}$ electrons/m^2) (Wanninger, 1993). As discussed by Adewale et al. (2012), the VTEC is calculated using the slant TEC (sTEC):

$$\mathrm{VTEC} = \frac{\mathrm{sTEC} - (B_R + B_S)}{M(E)} \tag{1}$$

where B_R is the interfrequency differential receiver biases and B_S the interfrequency differential satellite biases. According to Adewale et al. (2012) and Tiwari et al. (2013), the mapping function $M(E)$ employed is derived by the following equation:

$$M(E) = \frac{1}{\mathrm{COS}(Z')} = \left[1 - \left(\frac{R_E \times \mathrm{COS}(E)}{R_E + H_S}\right)^2\right]^{-1/2} \tag{2}$$

where Z' is the zenith angle of the satellite as seen from the observing station, H_S is the ionospheric pierce point altitude, normally taken as the F region peak, R_E is the radius of the Earth ($\sim$ 6378.1 km), and E is the elevation angle in radians.

Phase fluctuations are defined by the rate of change of TEC (ROT) in units of TEC/min which can indeed detect the presence of

Table 1
Details of the digital ionosonde (DI) and Global Positioning System (GPS) sites used in the present study.

American sector						
Location	Symbol used (Network)	Observations	Geog. Lat	Geog. Long.	Dip. Lat.	Local Time (LT)
Greenbelt, United States	GODE(IGS)	GPS	39.0 °N	76.8 °W	48.5 °N	LT=UT−5 h
Cambridge, United States	HNPT(IGS)	GPS	38.6 °N	76.1 °W	47.9 °N	LT=UT−5 h
Virgin Islands, United States	CRO1 (IGS)	GPS	17.6 °N	64.6 °W	24.8 °N	LT=UT−4 h
São Luís, Brazil	SL (INPE)	DI	2.33 °S	44.6 °W	02.4 °S	LT=UT−3 h
Eusebio, Brazil	BRFT (IGS)	GPS	03.9 °S	38.4 °W	07.4 °S	LT=UT−3 h
Iquitos, Peru	IQUI (SIRGAS)	GPS	03.8 °S	73.3 °W	07.5 °S	LT=UT−5 h
Fortaleza, Brazil	FZ (INPE)	DI	04.0 °S	38.0 °W	07.7 °S	LT=UT−3 h
Jicamarca, Peru	JIC	DI	12.0 °S	76.8 °W	0.08 °S	LT=UT−5 h
Arequipa, Peru	AREQ (IGS)	GPS	16.5 °S	71.5 °W	04.4 °S	LT=UT−5 h
Cachoeira Paulista, Brazil	CHPI (IGS)	GPS	22.7 °S	45.0 °W	19.4 °S	LT=UT−3 h
Copiapo, Chile	COPO (IGS)	GPS	27.4 °S	70.4 °W	14.1 °S	LT=UT−5 h
La Plata, Argentina	LPGS (IGS)	GPS	34.9 °S	57.9 °W	22.2 °S	LT=UT−4 h
Concepcion, Chile	CONZ (IGS)	GPS	36.8 °S	73.0 °W	21.3 °S	LT=UT−5 h
Port Stanley	PST	DI	51.6 °S	57.9 °W	31.5 °S	LT=UT−4 h
Rio Grande, Argentina	RIO2 (IGS)	GPS	53.8 °S	67.8 °W	32.1 °S	LT=UT−4 h
African sector						
Location	Symbol used (Network)	Observations*	Geog. Lat	Geog. Long.	Dip. Lat.	Local Time (LT)
Dakar, Senegal	DAKR (IGS)	GPS	14.7 °N	17.4 °W	05.0 °N	LT=UT−1 h
Addis Ababa, Ethiopia	ADIS (IGS)	GPS	09.0 °N	38.8 °E	01.2 °S	LT=UT+3 h
Cotonou, Benin	BJCO (IGS)	GPS	06.4 °N	02.5 °E	06.1 °S	LT=UT
Libreville, Gabon	NKLG (IGS)	GPS	00.4 °N	09.7 °E	13.7 °S	LT=UT+1 h
Mbarara, Uganda	MBAR (IGS)	GPS	00.6 °S	30.7 °E	12.2 °S	LT=UT+2 h
Lusaka, Zambia	ZAMB (IGS)	GPS	15.4 °S	28.3 °E	32.1 °S	LT=UT+2 h
Windhoek, Namibia	WIND (IGS)	GPS	22.6 °S	17.1 °E	42.4 °S	LT=UT+1 h
Springbok, South Africa	SBOK (IGS)	GPS	29.7 °S	17.9 °E	46.1 °S	LT=UT+1 h
Sutherland, South Africa	SUTH (IGS)	GPS	32.4 °S	20.8 °E	45.8 °S	LT=UT+1 h

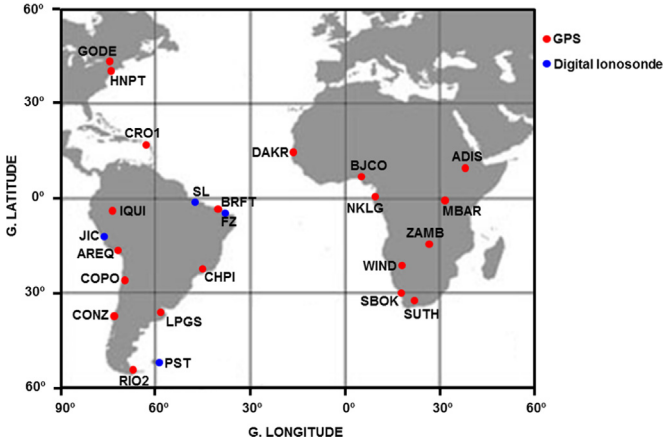

Fig. 2. Map showing the locations of the digital ionosonde and GPS stations, used in the present investigation.

the large scale ionospheric irregularities of the order of kilometers (Aarons, 1997; Aarons et al. 1997). The ROT is given by the equation (Warnant and Pottiaux, 2000; Chandra et al. 2009):

$$\mathrm{ROT}_{\mathrm{R}}^{\mathrm{S}}(t_i) = \frac{\mathrm{TEC}_{\mathrm{R}}^{\mathrm{S}}(t_i) - \mathrm{TEC}_{\mathrm{R}}^{\mathrm{S}}(t_{i-1})}{t_i - t_{i-1}} \quad (3)$$

with $\mathrm{ROT}_{\mathrm{R}}^{\mathrm{S}}(t_i)$=rate of TEC calculated at time epoch t_i by receiver (R) on satellite (S). Where $\mathrm{TEC}_{\mathrm{R}}^{\mathrm{S}}(t_i)$ and $\mathrm{TEC}_{\mathrm{R}}^{\mathrm{S}}(t_{i-1})$=TEC measured by receiver (R) on satellite (S) at epoch t_i and epoch t_{i-1} respectively.

According to Aarons et al. (1996), ionospheric amplitude scintillations are due to the scattering ionospheric irregularities of the order of several hundred meters to a kilometer. The S_4 index is normally used to monitor the ionospheric amplitude scintillations (Yeh and Liu, 1982; Basu et al., 1999; Li et al., 2008; Deng et al., 2013). As discussed by Yeh and Liu (1982), S_4 index is obtained by the normalized standard deviation of the received signal power intensity:

$$S_4^2 = \frac{\langle I^2 \rangle - \langle I \rangle^2}{\langle I \rangle^2} \quad (4)$$

where I is the signal power amplitude, and the brackets $\langle\rangle$ representing the time average values.

Fig. 2 shows the locations of the digital ionosondes and GPS receiving stations used in the present investigation. Table 1 provides the details of the digital ionosonde and GPS stations used in the present study. The São Luis (SL) and Fortaleza (FZ) stations belong to the "Instituto Nacional de Pesquisas Espaciais" (INPE) network. The Jicamarca and Port Stanley data were obtained from the Digital Ionogram DataBase (DIDBase) by the site http://ulcar.uml.edu/DIDBase/. The Greenbelt (GODE), Cambridge (HNPT), Virgin Islands (CRO1), Eusebio (BRFT), Arequipa (AREQ), Cachoeira Paulista (CHPI), Copiapo (COPO), La Plata (LPGS), Concepcion (CONZ), Rio Grande (RIO2), Dakar (DAKR), Addis (ADIS), Cotonou (BJCO), Libreville (NKLG), Mbarara (MBAR), Lusaka (ZAMB), Windhoek (WIND), Springbok (SBOK) and Sutherland (SUTH) stations belong to the International GNSS Service (IGS) for Geodynamics. The Iquitos (IQUI) station belong to the "Sistema de Referência Geocêntrico para as Américas" (SIRGAS). In addition, several global ionospheric TEC maps produced at the Massachusetts Institute of Technology (MIT) Haystack Observatory were obtained from http://www.haystack.mit.edu/.

Averages of the VTEC and ionospheric parameters (h′F and foF2) for four geomagnetically quiet days (with geomagnetic index $K_P < 3$) during September (days 27 and 28) and October (days 04 and 05) 2012 were calculated to compare with the observations obtained during the geomagnetically disturbed period.

The *Kp* index used in the present study was obtained from the website http://ftp.gwdg.de./pub/geophys/kp-ap/tab/. The Dst and

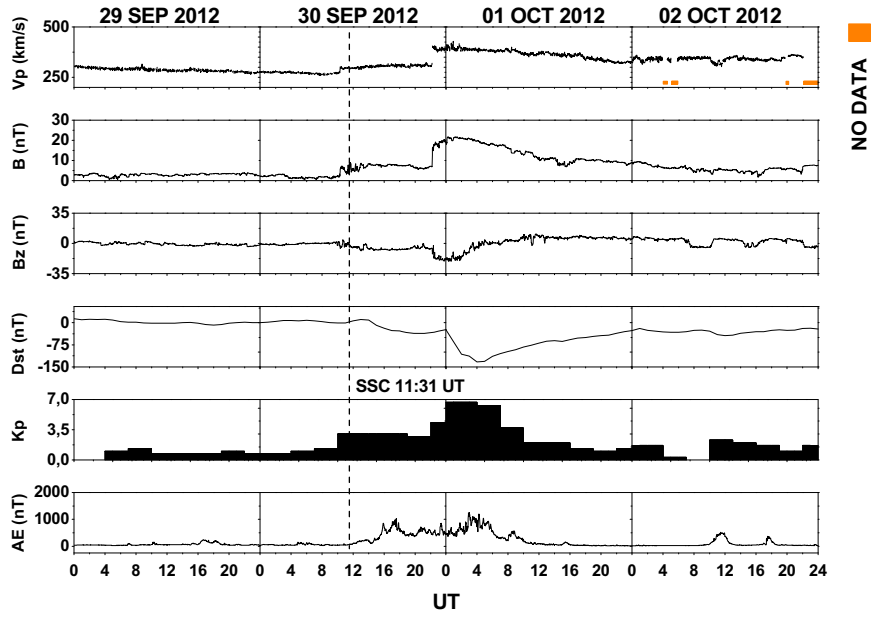

Fig. 3. Solar wind velocity (*Vp*), total interplanetary magnetic field (IMF) *B*, and *z* component of IMF *Bz*, for the period 29 September–02 October 2012. Also, the Dst, *Kp* and AE geomagnetic indices during the period 29 September–02 October 2012 are presented. The black vertical dashed line indicates the time of sudden storm commencement (SSC).

AE indices were got from http://wdc.kugi.kyoto-u.ac.jp/dstdir/ and the solar wind speed (*Vp*), and interplanetary magnetic field (IMF) (total magnetic field B and IMF component *Bz*) were got from http://www.srl.caltech.edu/ACE/. The F10.7 flux values were obtained from the National Aeronautics and Space Administration (NASA) website http://omniweb.gsfc.nasa.gov/form/dx1.html.

Fig. 3 shows the *Vp*, IMF (total magnetic field B and IMF component *Bz*) and variations of the geomagnetic indices (AE, Dst and *Kp*) during the period 29 September–02 October 2012. The horizontal orange bars indicate no data. The black vertical dashed line indicates the time of sudden storm commencement (SSC). The SSC started at 11:31 UT on 30 September 2012, following the southward turning of IMF *Bz*. A sudden increase in solar wind speed and IMF total field occurred at 22:10 UT on 30 September 2012. The solar wind speed jumps from ~312 km/s to ~405 km/s. The total magnetic field magnitude shows an abrupt increase from ~7 nT to ~20 nT. The minimum value of $Bz = -20$ nT was reached at 23:46 UT on 30 September 2012. The minimum value of Dst index (-133 nT) was reached at 04:00 UT on 01 October 2012. After the SSC, during the storm main phase, the *Kp* index reached ~7 on 01 October 2012. The AE index jumps from values under 250 nT to values of more than 1000 nT during SSC. The increased AE activity lasts until 01 October 2012. Fig. 3 also shows an increase in the AE index twice on 2 October 2012 (the first increase occurred at ~11:00 UT and the second at ~17:00 UT). The two increases in the AE index that occurred on 02 October reached the maximum value

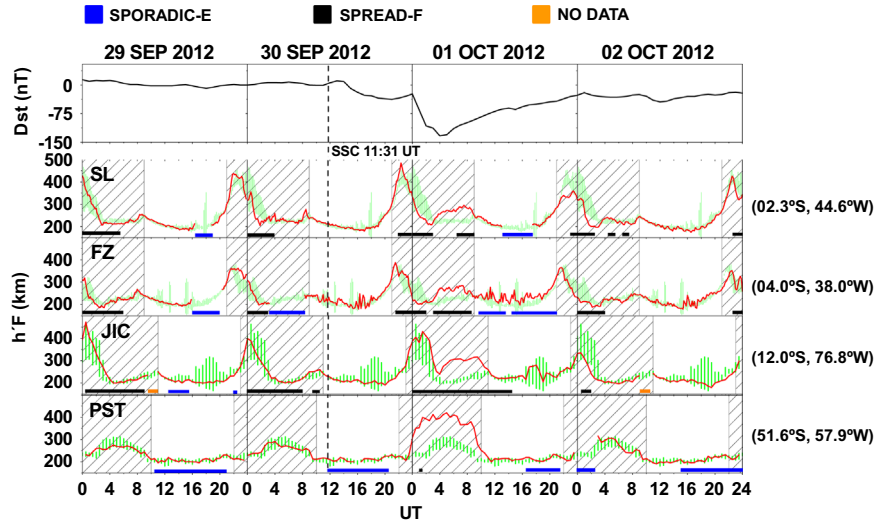

Fig. 4. Diurnal (UT) variations of the ionospheric parameter h´F (red lines) observed at JIC, SL, FZ and PST on the days 29, 30 September, 01 and 02 October 2012. It also shows the average of the observations on quiet days 27, 28 September, 04 and 05 October 2012 as green bands with ±1 standard deviation. The hatched portions indicate local nighttime periods (18:00–06:00 LT). Also, the diurnal (UT) variations of the Dst index for the period 29 September–02 October 2012 are presented. The black vertical dashed line indicates the time of SSC. The horizontal blue and black bars indicate periods when sporadic-E and spread-F occurred, respectively. The horizontal orange bars indicate no data. (For interpretation of the references to color in this figure legend, the reader is referred to the web version of this article.)

of ~500 nT and ~370 nT at 11:39 UT and 17:31 UT, respectively.

3. Results

Fig. 4 shows the variations of the ionospheric parameter, h′F (red lines), observed at SL, FZ, JIC and PST, covering the days on 29, 30 September, 01 and 02 October 2012. The black vertical dashed line indicates the time of SSC. The horizontal black and orange bars indicate spread-F and no data, respectively. The horizontal blue bars indicate the periods when sporadic-E occurred. Fig. 4 shows the average of the observations on quiet days 27, 28 September, 04 and 05 October 2012 as green bands with ±1 standard deviation. It also shows the Dst index variations during days 29 September–02 October 2012. The hatched portions indicate local nighttime periods (18:00–06:00 LT).

Fig. 4 shows that in general, on 29 and 30 September 2012 (geomagnetically quiet period; before SSC), the red lines (h′F) follow the average patterns at all stations. In Fig. 4 on the night of 30 September–01 October 2012 (during the end of main phase and first day of the recovery phase), SL, FZ (equatorial stations) (between ~03:00 UT and 09:00 UT), JIC (equatorial station) (between ~03:00 UT and 11:00 UT), and PST (mid-latitude station) (between ~23:00 UT and 11:00 UT) show h′F variations much larger than average variations, and this effect gradually increases from equatorial to mid-latitude stations. Fig. 4 shows small oscillations

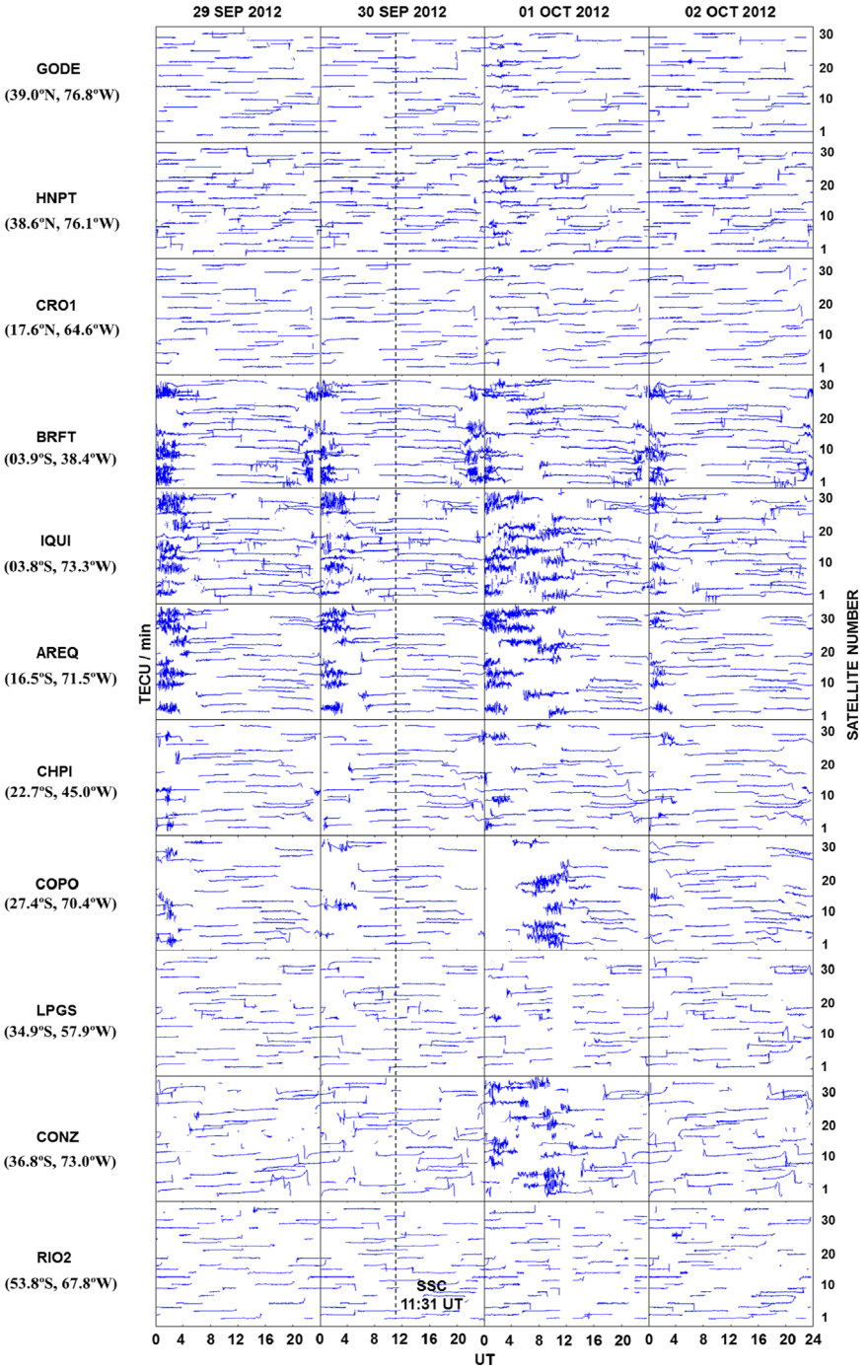

Fig. 5. The phase fluctuations from GPS signals obtained from different satellites at 11 receiving stations at American Sector during the period 29 September–2 October 2012. The black vertical dashed line indicates the time of SSC.

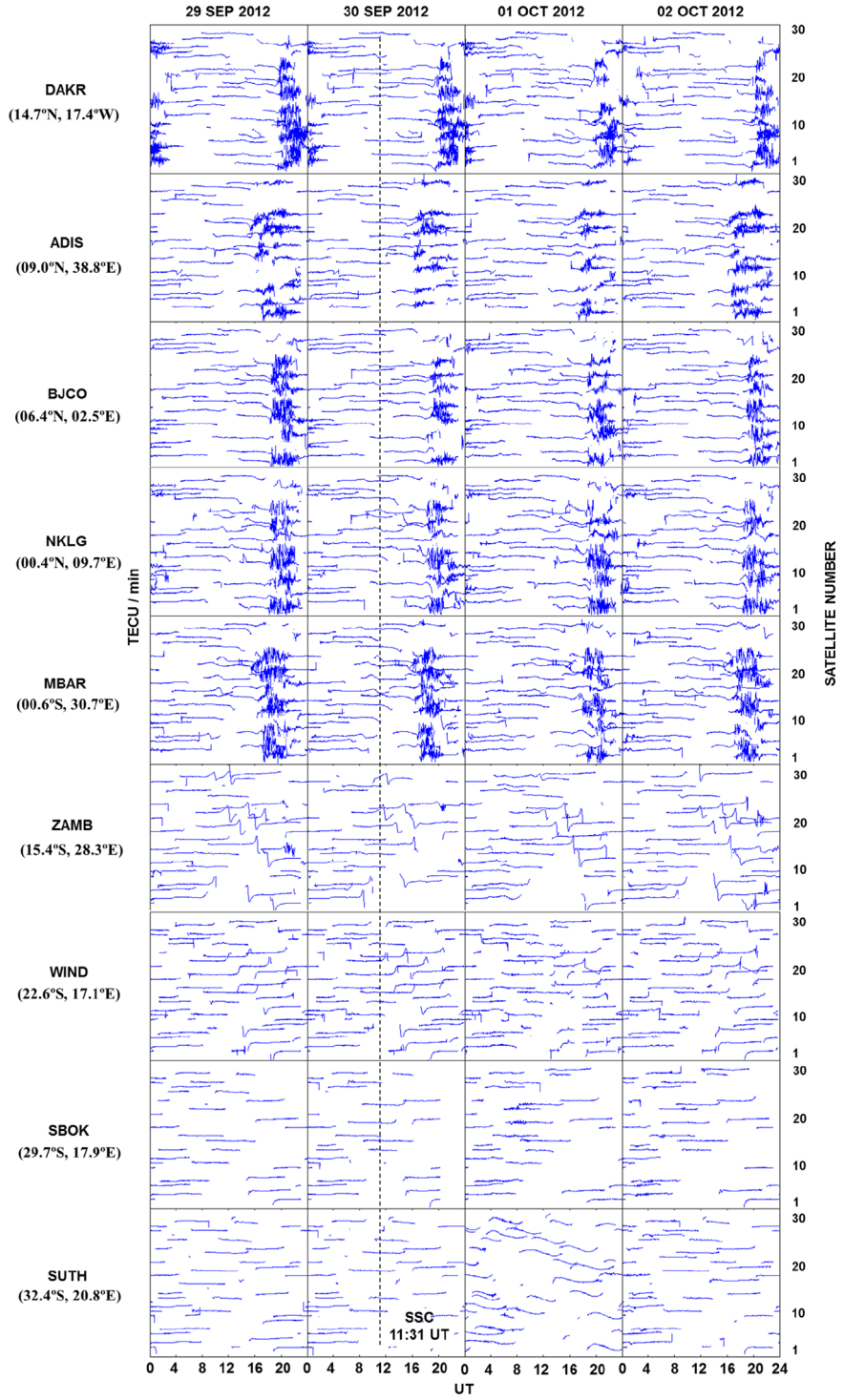

Fig. 6. The phase fluctuations from GPS signals obtained from different satellites at 9 receiving stations at African Sector during the period 29 September–02 October 2012. The black vertical dashed line indicates the time of SSC.

in h'F at FZ during the daytime period on 01 October 2012, due to the presence of sporadic-E. On the night of 01–02 October 2012 (recovery phase), Fig. 4 shows a decrease in the values of h´F at SL, FZ and JIC in relation to the geomagnetically quiet period.

Figs. 5 and 6 show the phase fluctuations (rate of change of TEC) observed (29, 30 September, 01 and 02 October 2012) at several GPS receiving stations located in the American and African sector, respectively. Figs. 7 and 8 show the amplitude scintillations for all satellites with elevation angles higher than 30° recorded in the American (at 11 receiving stations) and African (at 9 receiving stations) sectors, respectively. It should be mentioned that phase fluctuations and amplitude scintillations are due to large-scale ionospheric irregularities (of the order of kilometers) and small scale ionospheric irregularities (of the order of several hundred meters to a kilometer), respectively.

Figs. 4, 5 and 7 show the occurrence of ionospheric irregularities at equatorial and low- latitude stations (American sector) on the night of 28–29, 29–30 September (before SSC), 01–02 and 02–03 October 2012 (recovery phase). Figs. 4, 5 and 7 also show the occurrence of ionospheric irregularities on night of 30 September–01

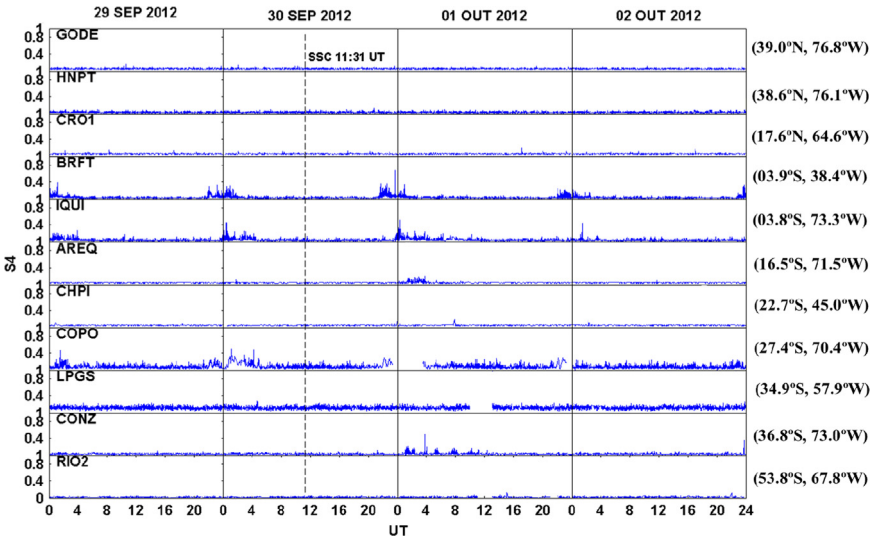

Fig. 7. GPS amplitude scintillations (S4 index) obtained from satellites (with elevation angles higher than 30°) at 11 receiving stations at American Sector during the period 29 September–02 October 2012.

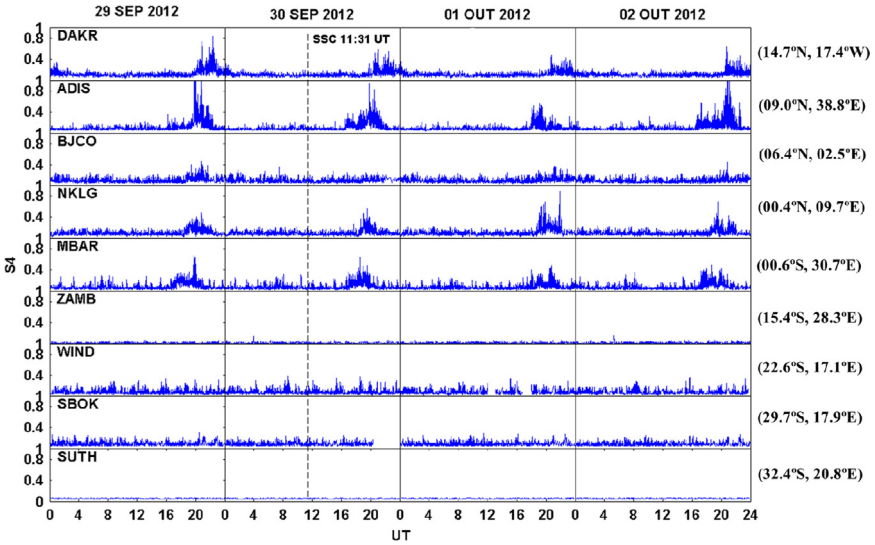

Fig. 8. GPS amplitude scintillations (S4 index) for the satellites with elevation angles higher than 30° at 9 receiving stations at African Sector on the days 29, 30 September, 01 and 02 October 2012.

October 2012 (main and recovery phase) at equatorial (SL, FZ, JIC, IQUI, and BRFT), low- (AREQ, CHPI and COPO) and mid- (CONZ and PST) latitude regions, in the American sector. Figs. 6 and 8 show phase fluctuations and amplitude scintillations (ionospheric irregularities), respectively, on the night of 29–30 September (before SSC), 30 September–01 October, 01–02 and 02–03 October 2012 (during geomagnetic storm period) at DAKR, ADIS, BJCO (equatorial stations), NKLG and MBAR (low-latitude stations), in the African sector.

Fig. 9 shows the variations of the ionospheric parameter, foF2 (red lines), observed at SL, FZ, JIC and PST, for the period investigated (29 September–02 October 2012). The hatched portions indicate local nighttime periods (18:00–06:00 LT). The horizontal black bars indicate periods when spread-F occurred. The horizontal orange bars indicate no data. The averaged foF2 (four quiet days viz. 27, 28 September, 04 and 05 October 2012) variations are shown as green bands and their widths correspond to ± 1 standard deviations. Also, Fig. 9 shows the time variations of the Dst index covering the days on 29, 30 September, 01 and 02 October 2012. Fig. 9 also shows the times when sporadic-E occurred (the horizontal blue bars). On 30 September (at 11:31 UT), the black vertical dashed line indicates the time of the SSC. The variations of the foF2 observed on 29, 30 September, 01 and 02 October 2012 are discussed later with VTEC observations.

Figs. 10 and 11 present the average VTEC variations from GPS observations in UT at several receiving stations during the period from 29, 30 September, 01 and 02 October 2012 (red lines), located in the American and African sector, respectively. The black vertical dashed line (on September 30, 2012) indicates the time of the SSC. It also shows the average of the observations on quiet days 27, 28 September, 04 and 05 October 2012 as green bands with ± 1 standard deviation. The gray areas indicate local nighttime periods (18:00–06:00 LT). At the top of Figs. 10 and 11 are shown the Dst index variations on the days 29, 30 September 2012, 01 and 02 October 2012.

In Figs. 9 and 10, during the main phase of the geomagnetic storm, a positive ionospheric storm is observed in the mid-latitudes regions (GODE, HNPT, CRO1, RIO2 and PST) during daytime on 30 September 2012. The foF2 variations (see Fig. 9) at SL and FZ (equatorial stations) show a negative ionospheric storm during the daytime on 30 September (main phase). On the night of 30 September–01 October between ~22:00 and 23:00 UT (main phase) a

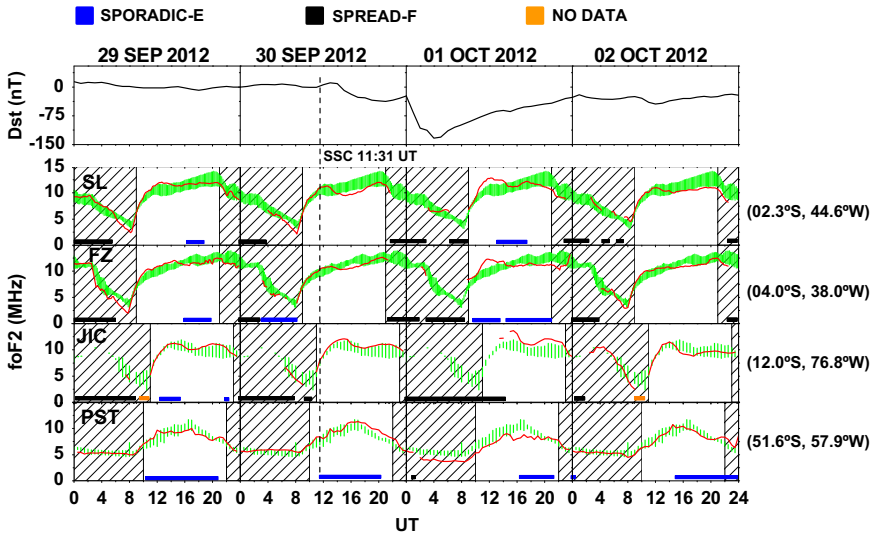

Fig. 9. Diurnal (UT) variations of the ionospheric parameter foF2 (red lines) observed at JIC, SL, FZ and PST on the days 29, 30 September, 01 and 02 October 2012. Also, the Dst index for the period 29 September–02 October 2012 are presented. The black vertical dashed line indicates the time of SSC. It also shows the average of the observations on quiet days 27, 28 September, 04 and 05 October 2012 as green bands with ± 1 standard deviation. The horizontal blue bars indicate sporadic-E. The horizontal orange bars indicate no data. The horizontal black bars indicate periods when spread-F occurred. The hatched portions indicate local nighttime periods (18:00–06:00 LT). (For interpretation of the references to color in this figure legend, the reader is referred to the web version of this article.)

slight positive ionospheric storm is observed at CHPI (low-latitude station; see Fig. 10). Also, on the night of 30 September–01 October (between ~00:00 and 03:30 UT) during the end of main phase, a negative ionospheric storm is observed at IQUI and AREQ (equatorial stations; see Fig. 10). Fig. 9 also shows a negative ionospheric storm at PST (mid-latitude station) on the night of 30 September–01 October. The VTEC variations at IQUI (see Fig. 10) show a positive ionospheric storm between ~04:00 UT and 07:00 UT on the night of 30 September–01 October in the recovery phase. Also, during the recovery phase (see Figs. 9 and 10), a positive ionospheric storm is observed closer to 12:00 UT on 01 October 2012 (daytime) at CRO1 (mid-latitude station), IQUI, SL, FZ, JIC (equatorial stations), CHPI and COPO (low-latitude stations), and the effect increasing from equatorial region to low-latitude region. During the daytime on 01 October (recovery phase), a negative ionospheric storm is observed (see Figs. 9 and 10) in the equatorial (FZ), low- (CHPI) and mid-latitudes regions (GODE, HNPT, CRO1, LPGS, CONZ and PST). On the night of 01-02 October (recovery phase), the VTEC variations (see Fig. 10) show a positive ionospheric storm at BRFT, IQUI and AREQ (equatorial stations). A positive ionospheric storm is also observed closer to 22:00 UT on 02 October 2012 at CHPI, COPO and CONZ.

Fig. 11 shows the variability of VTEC at equatorial, low- and mid-latitude regions in the African sector during the period 29 September–02 October 2012. Fig. 11 shows that on 01 October 2012 (the whole day) during the end of main phase and first day of the recovery phase, intense oscillations of the VTEC are observed at SUTH (mid-latitude station). Also, the VTEC variations show, in general, positive ionospheric storm at SUTH on 01 October 2012. A perusal of VTEC data obtained at different stations in Fig. 11 (African Sector) indicates that a long-duration positive ionospheric storm (over 6 h of enhancement) is observed during the daytime

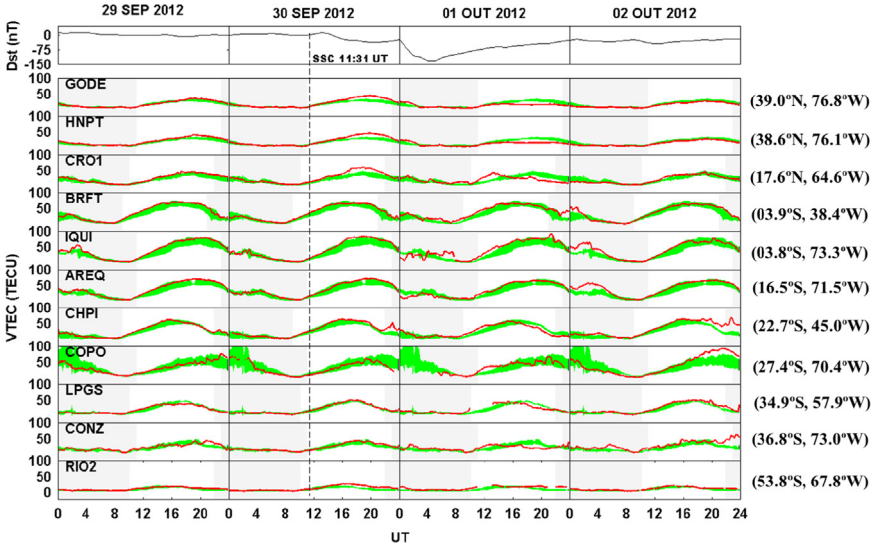

Fig. 10. Diurnal (UT) variations of the vertical total electron content (*VTEC*) measured using different satellites at American sector (11 receiving stations) during the period 29 September–02 October 2012 (red lines). The green bands are ± 1 standard deviation of the average quiet day (27, 28 September, 04 and 05 October 2012) values. The black vertical dashed line indicates the time of SSC. The gray areas indicate local nighttime periods (18:00–06:00 LT). Also, UT variations of the geomagnetic index Dst on the days 29, 30 September, 01and 02 October 2012 are presented.

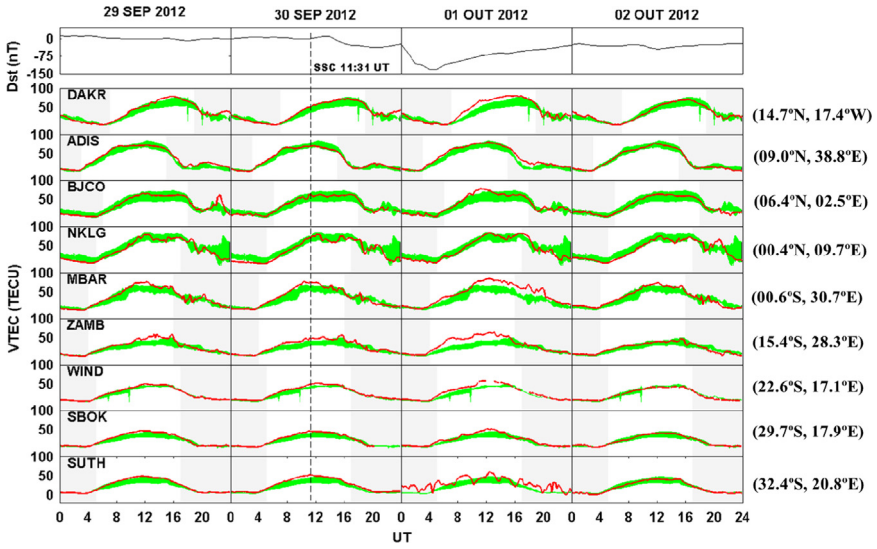

Fig. 11. Diurnal (UT) variations of the vertical total electron content (VTEC) measured using different satellites at African sector (9 receiving stations) during the period 29 September–02 October 2012 (red lines). Also, UT variations of the geomagnetic index Dst for the period 29 September–02 October 2012 are presented. The gray areas indicate local nighttime periods. The black vertical dashed line indicates the time of SSC. The green bands are ± 1 standard deviation of the average quiet day (four days) values. (For interpretation of the references to color in this figure legend, the reader is referred to the web version of this article.)

on 01 October 2012 (recovery phase) at DAKR (a near equatorial station), MBAR (a low-latitude station), ZAMB and WIND (mid-latitude stations). Also, during the daytime on 01 October 2012 (between ~10:00 UT and 12:00 UT), a slight positive ionospheric storm is observed at BJCO (a near equatorial station). A slight positive ionospheric storm is also observed between ~17:00 UT and 18:00 UT on the night of 01–02 October (recovery phase) at ADIS.

Fig. 12 shows GPS-TEC maps produced by MIT Haystack Observatory, observed at 12:00, 14:00, 16:00, 18:00, 20:00 and 22:00 UT on 29 (quiet day), 30 September and 01 October (geomagnetically disturbed conditions) 2012. In Fig. 12, the comparative analysis between geomagnetically quiet period (29/09/2012) and disturbed period (30/09/2012 and 01/10/2012) shows that the electron densities are higher (in the American and African sector) during the disturbed days. This analysis corroborates our results shown in Figs. 9, 10 and 11.

4. Discussion

The solar wind-magnetosphere dynamo, during intense geomagnetic storms, results in a large amount of energy dissipated at high latitudes (Tsurutani et al., 1997; Schunk and Nagy, 2000). This energy intensifies the electric current at high latitudes, resulting in Joule heating (Buonsanto, 1999). The Joule heating causes changes in the global thermospheric wind circulation. This Joule heating can also generate the atmospheric gravity waves (AGWs) (Hunsucker, 1982). Propagating through the thermosphere, AGWs produce traveling atmospheric disturbances (TADs) (Lee et al., 2002; Sahai et al., 2009c; Buonsanto, 1999). However, when the TADs interact with the ionosphere, they result in the generation of TIDs.

The TIDs can cause changes in the height of the ionosphere (Lee et al., 2002; de Jesus et al. 2012). Lee et al. (2002) have reported h′F variations much larger than the average variations at Wuhan (30.6 °N, 114.4 °E) and Chung-Li (24.9 °N, 121 °E) during the geomagnetic storm on 06–07 April 2000 due to the TID passage. de Jesus et al. (2012) have also observed an unusual uplifting of F-region (h′F) at Palmas (10.2 °S, 48.2 °W), São José dos Campos (23.2 °S, 45.9 °W) and Okinawa (26.3 °N, 127.8 °E) during the geomagnetic storm on 24–25 August 2005 due to the propagation of TIDs. In the present investigation, on the night of 30 September– 01 October, Fig. 4 shows an unusual uplilfting of the F-region (h′F) at SL, FZ (between ~03:00 UT and 09:00 UT), JIC (between ~03:00 UT and 11:00 UT), and PST (between ~23:00 UT and 11:00 UT) possibly related with TIDs caused by Joule heating at high latitudes (Lee et al., 2002; de Jesus et al., 2012). The possible passage of a TID at PST and JIC occurred at ~23:30 UT on 30 September and ~04:00 UT on 01 October 2012, respectively (see Fig. 4). Considering that the distance (in latitude) between PST and JIC is about 4610 km, this gives a velocity of propagation of about 1024 km/h (or 284 m/s) for TID. On 01 October, JIC (see Fig. 4) shows two peaks (at h′F) at about 07:00 UT and 09:30 UT, respectively. Considering that the period between these two peaks is 2.5 h, this gives a wavelength of about 2560 km for TID. These values found are consistent with large scale TIDs (Hunsucker, 1982; Hocke and Schlegel, 1996). It should be mentioned that Fig. 3 shows large enhancements in the AE index on 30 September and 01 October 2012 (during the main and recovery phases of the storm), indicating that a large amount of energy was injected into the auroral zone, and can produce TIDs by Joule heating (Hunsucker, 1982; Buonsanto, 1999).

On the nights of 29–30 September (quiet period; before SSC), and 30 September–01 October (main phase), the observations (see Fig. 4) show that around pre-reversal enhancement time (nearly 23:00 UT) the variations in h′F at SL and JIC follow the variations of the quiet period (used as reference). However, on the night of 01–02 October (recovery phase), the pre-reversal uplifting of the F region at SL and JIC is smaller than the average patterns. According to Abdu (1997), the small pre-reversal uplifting of the F region is related with the disturbance thermospheric winds or disturbance electric fields.

The ionospheric response during geomagnetic storms at equatorial, low- and mid-latitude regions in the American sector has been investigated by de Abreu et al. (2010b), and de Jesus et al. (2010, 2013). de Abreu et al. (2010b) and de Jesus et al. (2010, 2013) have investigated the ionospheric response during intense geomagnetic storms which occurred on 07–08 September 2002, 14–15 December 2006 and 24–25 October 2011, respectively, using ionospheric sounding data and GPS observations. de Abreu et al. (2010b) and de Jesus et al. (2013) have observed strong negative

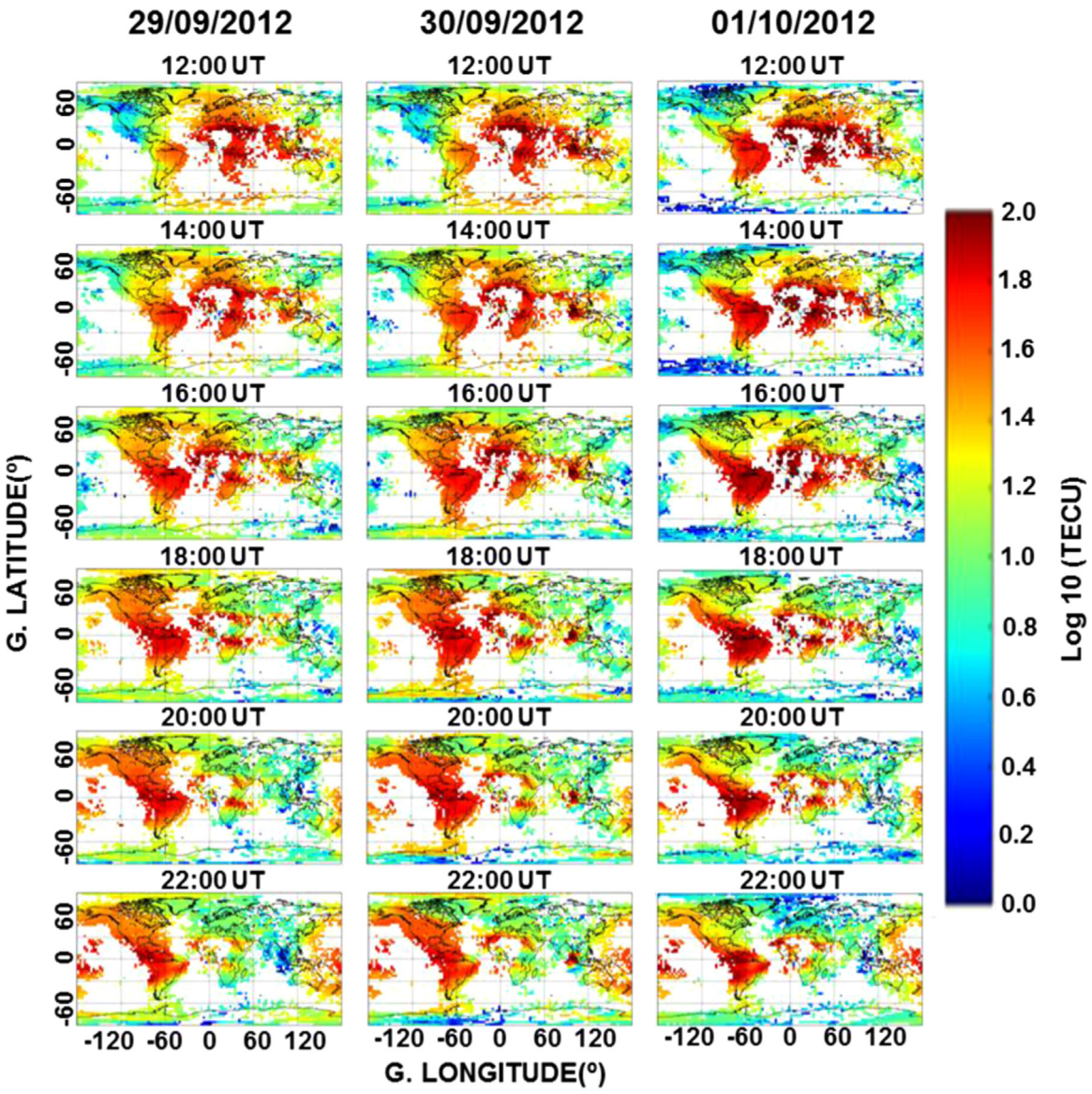

Fig. 12. Global GPS-TEC maps during the geomagnetically quiet period on 23 September 2012, and geomagnetically disturbed days of 30 September and 01 October 2012.

ionospheric storm at mid-latitude regions in the American sector during the geomagnetic storm in September 2002 and October 2011, respectively. de Jesus et al. (2010) have also reported a negative ionospheric storm at low- and mid-latitude stations in the American sector during the storm in December 2006. In the present investigations, Figs. 9 and 10 show strong negative ionospheric storms at equatorial (SL and FZ), low- (CHPI) and mid- (GODE, HPNT, CRO1, LPGS, CONZ, and PST) latitude regions in the American sector on 01 October 2012. These negative ionospheric storms observed in the American sector are possibly related with an O/N_2 density ratio decrease (Prolss, 1980, 1997; Danilov and Morozova, 1985; Danilov, 2013). The present results on 01 October 2012 confirm the observations during other intense geomagnetic storms investigated by de Abreu et al. (2010b), and de Jesus et al. (2010, 2013).

Some researchers have investigated the response of the ionosphere F region in the American and African sector during the occurrence of geomagnetic storms (Mansilla and Zossi, 2013; de Abreu et al., 2014). Mansilla and Zossi (2013) have analyzed the ionospheric response to the 03 August 2010 geomagnetic storm in the Asian, European, African and American sector, using data from ionosonde stations located at mid-latitude. de Abreu et al. (2014) have investigated ionospheric response to two moderate geomagnetic storms (which occurred in May 2010) using GPS-TEC measurements in the South American (equatorial, low- and mid-latitude regions) and African (low- and mid-latitude regions) sectors. de Abreu et al. (2014) have observed positive ionospheric storms during daytime hours at equatorial, low- and mid-latitude stations in the South American and African sectors during geomagnetic storms which occurred in May 2010. Mansilla and Zossi (2013) have reported positive ionospheric storms at mid-latitude stations in the American and African sectors during a moderate geomagnetic storm which occurred on 03–05 August 2010. According to de Abreu et al. (2014), the positive ionospheric storms observed in the American and African sectors are associated with the equatorward thermospheric wind. In addition, according to Namgaladze et al., 2000, positive ionospheric storms are related with large-scale neutral wind circulations and the passage of TIDs. In the present investigations, the observations (see Figs. 9, 10 and 11) also show positive ionospheric storms in the American and African sectors during geomagnetic storm which occurred on 30 September–02 October 2012. On 30 September, Figs. 9 and 10 show positive ionospheric storms at low- (CHPI) and mid- (PST, GODE, HNPT, CRO1 and RIO2) latitude stations in the American

sector. Fig. 9 (foF2 variations) also shows that at SL, FZ, and JIC (equatorial stations) have pronounced electron density enhancements during the daytime on 01 October 2012. The VTEC variations (see Figs. 10 and 11) also show positive ionospheric storms at equatorial, low- and mid-latitude stations in the American (on 01 and 02 October) and African (on 01 October) sectors. These positive ionospheric storms observed in the American and African sectors (on September–October 2012) are probably associated with the equatorward thermospheric wind, large-scale neutral wind circulations and the passage of TIDs (Namgaladze et al., 2000; Prolss, 1993; Balan et al., 2009, 2010; Mansilla and Zossi, 2013; de Abreu et al., 2014). The present results confirm the observations during other geomagnetic storms investigated by Mansilla and Zossi (2013), and de Abreu et al. (2014). In the present investigation, Fig. 11 also shows intense oscillations in the VTEC observations at SUTH on 01 October 2012, possibly associated with the passage of TID (Namgaladze et al., 2000; Prolss, 1993).

Ngwira et al. (2012) have investigated the response of the ionospheric F-layer in the mid-latitude region in the South African sector during the intense geomagnetic storms which occurred on 24–27 July 2004, using ionospheric sounding data and GPS observations. Ngwira et al. (2012) have reported a long-duration positive ionospheric storm at mid-latitude region in the South African sector on 25 and 27 July 2004, associated with large-scale wind circulations and equatorward neutral winds. Ngwira et al. (2012) classified as a long-duration positive ionospheric storm when the increase of the ionospheric electron density (positive ionospheric storm) lasted over 6 h. Mansilla and Zossi (2013) have also observed a long-duration positive ionospheric storm (over 6 h of enhancement) at mid-latitude stations in the African sector during the moderate geomagnetic storm that occurred on 03–05 August 2010. In the present study, a perusal of foF2 and VTEC data obtained at different stations in the American sector (Figs. 9 and 10) show long-duration positive ionospheric storms (over 6 h of enhancement) at mid-latitude stations (GODE, HNPT, CRO1, RIO2 and PST) during the daytime on 30 September (main phase). Fig. 11 also shows long-duration positive ionospheric storms (over 6 h of enhancement) at DAKR (a near equatorial station), MBAR (a low-latitude station), ZAMB, WIND and SUTH (mid-latitude stations) during the daytime on 01 October, in the recovery phase. These five stations (DAKR, MBAR, ZAMB, WIND and SUTH) are located in the African sector. These long-duration positive ionospheric storms observed in the American (on 30 September) and African (on 01 October) sector are possibly related with equatorward neutral winds and large-scale wind circulations (Ngwira et al., 2012). The present results on 30 September and 01 October 2012 confirm the observations during other geomagnetic storms studied by Ngwira et al. (2012), and Mansilla and Zossi (2013).

As discussed by Whalen (2002), the equatorial ionospheric irregularities receive distinct denominations according to their latitudinal extent in relation to the magnetic equator. According to Whalen (2002), the ionospheric irregularity that is confined below the F region maximum and can be detected only by the ionospheric sounding observation at and near the magnetic equator, receive the name of bottomside spread-F. Equatorial ionospheric irregularities rise to high altitude, extends via the magnetic field to higher latitudes and can be observed by the ionospheric sounders located in the equatorial and low-latitude regions (Abdu et al., 1991,Whalen, 2002).

Figs. 4, 5 and 7 indicate that on the night of 28–29, 29–30 September (before SSC), 30 September–01 October and 01–02 October 2012 (disturbed period) during the pre-reversal period resulted in the generation of equatorial ionospheric irregularities (equatorial and low-latitude stations), in the American sector. On the night of 02–03 October 2012, Fig. 4 shows the generation of bottomside spread-F at SL and FZ (equatorial stations). Figs. 6 and 8 show the generation of equatorial ionospheric irregularities in the African sector (equatorial and low-latitude regions) on the night of 29–30 September (before SSC), 30 September–01 October, 01–02 and 02–03 October 2012 (geomagnetic storm period). The generation of equatorial ionospheric irregularity is associated with the rapid upward motion of the ionospheric F layer and development of the Rayleigh–Taylor instability (Sultan, 1996; Martinis et al., 2005). de Abreu et al. (2014) have reported no generation of ionospheric irregularities (in the South American and African sectors) before and during the moderate geomagnetic storms that occurred in May 2010. However, in the present investigation, it is observed the generation of equatorial ionospheric irregularities, in the American and African sectors, before and during the intense geomagnetic storm that occurred in September–October 2012. These discrepancies between the results observed by de Abreu et al. (2014) (before and during the geomagnetic storms of May 2010) and the results presented in this investigation (before and during the geomagnetic storm of September–October 2012) are associated with seasonal occurrence of ionospheric irregularities in the American and African sectors (Abdu et al., 1983, 1985; Sahai et al., 1994, 2000; Paznukhov et al., 2012; Akala et al., 2014).

Figs. 4 and 5 show the generation of equatorial ionospheric irregularities in the South American sector (equatorial, low- and mid-latitude regions), on the night of 30 September–01 October 2012, possibly related with the prompt penetration of the magnetospheric electric field [during the decrease of *Bz* between about 22 UT (30 September) and 01 UT (01 October); see Fig. 3] that result to an unusual pre-reversal enhancement. However on this night (30 September–01 October), Fig. 6 shows the same type of irregularities observed before the geomagnetic storm in the African sector. Fig. 6 shows no irregularities at mid-latitudes in the African sector on the night of 30 September–01 October, possibly because there was no intensification of the pre-reversal enhancement (in the African sector) due to the prompt penetration of the magnetospheric electric field.

In the South American sector, some nights show the presence of phase fluctuations and absence of amplitude scintillations. Figs. 5 and 7 show the presence of phase fluctuations and absence of amplitude scintillations, respectively, on the nights of 28–29 (in AREQ and CHPI), 29–30 September (in AREQ), 01 October (in CHPI and COPO), and 01–02 October (in AREQ). This occurs because the phase fluctuations are associated to large scale irregularities, having the order of kilometers, and the amplitude scintillations are related to small scale irregularities, having the order of several hundred meters to a kilometer.

5. Conclusions

In this paper we have presented and analyzed the ionospheric sounding and GPS observations in the equatorial, low- and mid-latitude regions in the American and African sectors during the intense geomagnetic storm of 30 September–01 October 2012. This intense geomagnetic storm occurred during the period of high solar activity in the unusual solar cycle 24. Some of the salient features associated with these observations are summarized below:

1. On the geomagnetic disturbed night of 30 September–01 October, an unusual uplifting of the F layer was observed at SL, FZ, JIC (equatorial stations) and PST (mid-latitude stations) due to the propagation of TIDs generated by the Joule heating in the high-latitude region.
2. During the main phase of the geomagnetic storm (30 September) there was a long-duration positive ionospheric storm in

both mid-latitude American hemispheres, related with large-scale wind circulations and equatorward neutral winds. Also, during the recovery phase (01 and 02 October), positive ionospheric storms were observed, in the American sector at equatorial, low- and mid- latitude regions, related with an equatorward neutral wind and the passage of TIDs.

3. During the recovery phase of the geomagnetic storm (01 October), the African sector at equatorial, low- and mid-latitude regions showed a long-duration positive ionospheric storm due to large-scale neutral wind circulations, and equatorward neutral winds.
4. The foF2 variations at equatorial stations showed a slight negative ionospheric storm on 30 September (main phase) and 02 October (recovery phase). Also, during the recovery phase (on 01 October 2012) the foF2 variations and GPS–VTEC observations at equatorial (SL and FZ), low- (CHPI) and mid- (GODE, HPNP, CRO1, LPGS, CONZ and PST) latitude stations showed negative ionospheric storms in the American sector.
5. Equatorial ionospheric irregularities were observed in the South American sector on the night of 30 September–01 October 2012 (main and recovery phase) up to CONZ (mid-latitude station), after an unusual pre-reversal enhancement in the equatorial stations, associated with the prompt penetration of the magnetospheric electric field. Equatorial ionospheric irregularities were also observed at equatorial and low-latitude stations in the South American sector on the night of 28–29, 29–30 September (before SSC) and 01–02 October (recovery phase).
6. In the African sector there was no suppression of ionospheric irregularities due to occurrence of intense geomagnetic storm of September–October 2012. The same type of ionospheric irregularities observed during the quiet period (before SSC) were also observed during the disturbed period in the African sector.

Acknowledgments

Thanks are due to “Fundação de Amparo à Pesquisa do Estado de São Paulo” (FAPESP) for kindly providing financial support through process number 2011/21936-9. The authors also thank the authorities of the International GNSS Service (IGS), “Sistema de Referência Geocêntrico para as Américas” (SIRGAS), Massachusetts Institute of Technology (MIT) Haytack Observatory, Digital Ionogram DataBase (DIDBase), NASA, and “Instituto Nacional de Pesquisas Espaciais” (INPE), for easy access to their data.

References

Aarons, J., Mendillo, M., Yantosca, R., 1996. GPS phase fluctuations in the equatorial region during the MISETA 1994 campaign. J. Geophys. Res. 101, 26851–26862.
Aarons, J., 1997. Global positioning system phase fluctuations at auroral latitudes. J. Geophys. Res. 102, 17219–17231.
Aarons, J., Mendillo, M., Yantosca, R., 1997. GPS phase fluctuations in the equatorial region during sunspot minimum. Radio Sci. 32, 1535–1550. http://dx.doi.org/10.1029/97RS00664.
Abdu, M.A., de Medeiros, R.T., Nakamura, Y., 1983. Latitudinal and magnetic flux tube extension of the equatorial spread F irregularities. J. Geophys. Res. 88, 4861–4868.
Abdu, M.A., Sobral, J.H.A., Nelson, O.R., Batista, I.S., 1985. Solar cycle related range type spread-F occurrence characteristics over equatorial and low latitude station in Brazil. J. Atmos. Terr. Phys. 47, 901–905.
Abdu, M.A., Muralikrishna, P., Batista, I.S., Sobral, J.H.A., 1991. Rocket observations of equatorial plasma bubble over Natal, Brazil, using a high frequency capacitance probe. J. Geophys. Res. 96 (A5), 7689–7695.
Abdu, M.A., 1997. Major phenomena of the equatorial ionosphere-thermosphere system under disturbed conditions. J. Atmos. Sol. Terr. Phys. 59, 1505–1519.
Abdu, M.A., Jayachandran, P.T., MacDougall, J., Cecile, J.F., Sobral, J.H.A., 1998. Equatorial F region zonal plasma irregularity drifts under magnetospheric disturbances. Geophys. Res. Lett. 25, 4137–4140.
Adewale, A.O., Oyeyemi, E.O., Olwendo, J., 2012. Solar activity dependence of total electron content derived from GPS observations over Mbarara. Adv. Space Res. 50, 415–426. http://dx.doi.org/10.1016/j.asr.2012.05.006.
Akala, A.O., Amaeshi, L.L.N., Doherty, P.H., Groves, K.M., Carrano, C.S., Bridgwood, C. T., Seemala, G.K., Somoye, E.O., 2014. Characterization of GNSS scintillations over Lagos, Nigeria during the minimum and ascending phases (2009–2011) of solar cycle 24. Adv. Space Res. 53, 37–47.
Annakuliev, S.K., Deminov, M.G., Shubin, V.N., 2005. Storm semiempirical model in the ionosphere of middle latitudes [in Russian]. Sol. Terr. Phys. 8, 145–146.
Balan, N., Alleyne, H., Otsuka, Y., Lekshmi, V.D., Fejer, B.G., McCrea, I., 2009. Relative effects of electric field and neutral wind on positive ionospheric storms. Earth Planets Space 61, 439–445.
Balan, N., Shiokawa, K., Otsuka, Y., Kikuchi, T., Vijaya Lekshmi, D., Kawamura, S., Yamamoto, M., Bailey, G.J., 2010. A physical mechanism of positive ionospheric storms at low latitudes and midlatitudes. J. Geophys. Res. 115, A02304.
Basu, S., Groves, K.M., Quinn, J.M., Doherty, P., 1999. A comparison of TEC fuctuations and scintillations at Ascension Island. J. Atmos. Sol. Terr. Phys. 61, 1219–1226.
Basu, Su, Basu, S., Makela, J.J., Sheehan, R.E., MacKenzie, E., Doherty, P., Wright, J.W., Keskinen, M.J., Pallamraju, D., Paxton, L.J., Berkey, F.T., 2005. Two components of ionospheric plasma structuring at midlatitudes observed during the large magnetic storm of October 30, 2003 L12S06. Geophys. Res. Lett. 32. http://dx.doi.org/10.1029/2004GL021669.
Basu, Su, Basu, S., Makela, J.J., MacKenzie, E., Doherty, P., Wright, J.W., Rich, F., Keskinen, M.J., Sheehan, R.E., Coster, A.J., 2008. Large magnetic storm-induced nighttime ionospheric flows at midlatitudes and their impacts on GPS-based navigation systems. J. Geophys. Res. 113, A00A06. http://dx.doi.org/10.1029/2008JA013076.
Batista, I.S., de Paula, E.R., Abdu, M.A., Trivedi, N.B., Greenspan, M.E., 1991. Ionospheric effects of the March 13, 1989, magnetic storm at low and equatorial latitudes. J. Geophys. Res. 96 (A8), 13943–13952.
Batista, I.S., Abdu, M.A., Souza, J.R., Bertoni, F., Matsuoka, M.T., Camargo, P.O., Bailey, G.J., 2006. Unusual early morning development of the equatorial anomaly in the Brazilian sector during the Halloween magnetic storm. J. Geophys. Res. 111, A05307. http://dx.doi.org/10.1029/2005JA011428.
Batista, I.S., Abdu, M.A., Nogueira, P.A.B., Paes., R.R., Souza, J.R., Reinisch, B.W., Rios, V.H., 2012. Early morning enhancement in ionospheric electron density during intense magnetic storms. Adv. Space Res. 49, 1544–1552.
Borries, C., Jakowski, N., Wilken, V., 2009. Storm induced large scale TIDs observed in GPS derived TEC. Ann. Geophys. 27, 1605–1612.
Buonsanto, M.J., 1999. Ionospheric storms – a review. Space Sci. Rev. 88, 563–601.
Chandra, K.R., Srinivas, V.S., Sarma, A.D., 2009. Investigation of ionospheric gradients for GAGAN application. Earth Planets Space 61, 633–635.
Danilov, A.D., Morozova, L.D., 1985. Ionospheric storms in the F2 region. morphology and physics (Review). Geomag. Aeron. 25, 593–605.
Danilov, A.D., 2013. Ionospheric F-region response to geomagnetic disturbances. Adv. Space Res. 52 (3), 343–366. http://dx.doi.org/10.1016/j.asr.2013.04.019.
de Abreu, A.J., Sahai, Y., Fagundes, P.R., Becker-Guedes, F., de Jesus, R., Guarnieri, F.L., Pillat, V.G., 2010a. Response of the ionospheric F-region in the Brazilian sector during the super geomagnetic storm in April 2000 observed by GPS. Adv. Space Res. 45, 1322–1329. http://dx.doi.org/10.1016/j.asr.2010.02.003.
de Abreu, A.J., Fagundes, P.R., Sahai, Y., de Jesus, R., Bittencourt, J.A., Brunini, C., Gende, M., Pillat, V.G., Lima, W.L.C., Abalde, J.R., Pimenta, A.A., 2010b. Hemispheric asymmetries in the ionospheric response observed in the American sector during an intense geomagnetic storm. J. Geophys. Res. 115, A12312. http://dx.doi.org/10.1029/2010JA015661.
de Abreu, A.J., Fagundes, P.R., Sahai, Y., de Jesus, R., Bittencourt, J.A., Pillat, V.G., 2011. An investigation of ionospheric F region response in the Brazilian sector to the super geomagnetic storm of May 2005. Adv. Space Res. 48, 1211–1220. http://dx.doi.org/10.1016/j.asr.2011.05.036.
de Abreu, A.J., Fagundes, P.R., Gende, M., Bolaji, O.S., de Jesus, R., Brunini, C., 2014. Investigation of ionospheric response to two moderate geomagnetic storms using GPS-TEC measurements in the South American and African sectors during the ascending phase of solar cycle 24. Adv. Space Res. 53, 1313–1328. http://dx.doi.org/10.1016/j.asr.2014.02.011.
de Jesus, R., Sahai, Y., Guarnieri, F.L., Fagundes, P.R., de Abreu, A.J., Becker-Guedes, F., Brunini, C., Gende, M., Cintra, T.M.F., de Souza, V.A., Pillat, V.G., Lima, W.L.C., 2010. Effects observed in the ionospheric F-region in the South American sector during the intense geomagnetic storm of 14 December 2006. Adv. Space Res. 46, 909–920. http://dx.doi.org/10.1016/j.asr.2010.04.031.
de Jesus, R., Sahai, Y., Guarnieri, F.L., Fagundes, P.R., de Abreu, A.J., Bittencourt, J.A., Nagatsuma, T., Huang, C.-S., Lan, H.T., Pillat, V.G., 2012. Ionospheric response of equatorial and low latitude F-region during the intense geomagnetic storm on 24–25 August 2005. Adv. Space Res. 49, 518–529. http://dx.doi.org/10.1016/j.asr.2011.10.020.
de Jesus, R., Sahai, Y., Fagundes, P.R., de Abreu, A.J., Brunini, C., Gende, M., Bittencourt, J.A., Abalde, J.R., Pillat, V.G., 2013. Response of equatorial, low- and mid-latitude F-region in the American sector during the intense geomagnetic storm on 24–25 October 2011. Adv. Space Res. 52, 147–157. http://dx.doi.org/10.1016/j.asr.2013.03.017.
Deng, B., Huang, J., Liu, W., Xu, J., Huang, L., 2013. GPS scintillation and TEC depletion near the northern crest of equatorial anomaly over South China. Adv. Space Res. 51, 356–365.
Fejer, B.G., Scherliess, L., 1997. Empirical models of storm time equatorial zonal electric fields. J. Geophys. Res. 102, 20047–24056.
Foster, J.C., Rich, F.J., 1998. Prompt midlatitude electric field effects during severe geomagnetic storms. J. Geophys. Res. 103, 26367–26372. http://dx.doi.org/10.1029/97JA03057.

Foster, J.C., Rideout, W., 2005. Midlatitude TEC enhancements during the October 2003 superstorm L12S04. Geophys. Res. Lett. 32. http://dx.doi.org/10.1029/2004GL021719.
Foster, J.C., Rideout, W., Sandel, B., Forrester, W.T., Rich, F.J., 2007. On the relationship of SAPS to storm enhanced density. J. Atmos. Sol. Terr. Phys. 69, 303–313. http://dx.doi.org/10.1016/j.jastp.2006.07.021.
Gonzalez, W.D., Tsurutani, B.T., 1987. Criteria of interplanetary parameters causing intense magnetic storms (Dst < -100 nT). Planet. Space Sci. v. 35 (n. 9), 1101–1109.
Heelis, R.A., Sojka, J.J., David, M., Schunk, R.W., 2009. Storm time density enhancements in the middle-latitude dayside ionosphere. J. Geophys. Res. 114, A03315. http://dx.doi.org/10.1029/2008JA013690.
Hocke, K., Schlegel, K., 1996. A review of atmospheric gravity waves and traveling ionospheric disturbances: 1982–1995. Ann. Geophys. 14, 917–940.
Huang, C.-S., Foster, J.C., Goncharenko, L.P., Sofko, G.J., Borovsky, J.E., Rich, F.J., 2003. Midlatitude ionospheric disturbances during magnetic storms and substorms. J. Geophys. Res. 108 (A6), 1244. http://dx.doi.org/10.1029/2002JA009608.
Hunsucker, R.D., 1982. Atmospheric gravity waves generated in the high-latitude ionosphere: a review. Rev. Geophys. 20, 293–315. http://dx.doi.org/10.1029/RG020i002p00293.
Keskinen, M.J., Basu, Su, Basu, S., 2004. Midlatitude sub-auroral ionospheric small scale structure during a magnetic storm. Geophys. Res. Lett. 31 (9), L09811. http://dx.doi.org/10.1029/2003GL019368.
Klimenko, M.V., Klimenko, V.V., Ratovsky, K.G., Goncharenko, L.P., Sahai, Y., Fagundes, P.R., de Jesus, R., de Abreu, A.J., Vesnin, A.M., 2011. Numerical modeling of ionospheric effects in the middle- and low-latitude F region during geomagnetic storm sequence of 9–14 September 2005. Radio Sci. 46, RS0D03. http://dx.doi.org/10.1029/2010RS004590.
Lee, C.C., Liu, J.Y., Reinisch, B.W., Lee, Y., Liu, L., 2002. The Propagation of traveling atmospheric disturbances observed during the April 6–7, 2000 ionospheric storm. Geophys. Res. Lett. 29 (5), 1068. http://dx.doi.org/10.1029/2001GL013516.
Li, G., Ning, B., Zhao, B., Liu, L., Liu, J.Y., Yumoto, K., 2008. Effects of geomagnetic storm on GPS ionospheric scintillations at Sanya. J. Atmos. Sol. Terr. Phys. 70, 1034–1045.
Mansilla, G.A., Zossi, M.M., 2012. Thermosphere–ionosphere response to a severe magnetic storm: a case study. Adv. Space Res. 49, 1581–1586.
Mansilla, G.A., Zossi, M.M., 2013. Ionospheric response to the 3 August 2010 geomagnetic storm at mid and mid-high latitudes. Adv. Space Res. 51, 50–60.
Martinis, C.R., Mendillo, M.J., Aarons, J., 2005. Toward a synthesis of equatorial spread F onset and suppression during geomagnetic storms. J. Geophys. Res. 110, A07306.
Namgaladze, A.A., Forster, M., Yurik, R.Y., 2000. Analysis of the positive ionospheric response to a moderate geomagnetic storm using a global numerical model. Ann. Geophys. 18, 461–477.
Ngwira, C.M., McKinnell, L.A., Cilliers, P.J., Coster, A.J., 2012. Ionospheric observations during the geomagnetic storm events on 24–27 July 2004: long-duration positive storm effects. J. Geophys. Res. 117, A00L02.
Pavlov, A.V., 1994. The role of vibrationally excited nitrogen in the formation of the mid-latitude negative ionospheric storms. Ann. Geophys. 12, 554–564.
Paznukhov, V.V., Carrano, C.S., Doherty, P.H., Groves, K.M., Caton, R.G., Valladares, C. E., Seemala, G.K., Bridgwood, C.T., Adeniyi, J., Amaeshi, L.L.N., Damtie, B., Mutonyi, F.D., Ndeda, J.O.H., Baki, P., Obrou, O.K., Okere, B., Tsidu, G.M., 2012. Equatorial plasma bubbles and L-band scintillations in Africa during solar minimum. Ann. Geophys. 30, 675–682.
Prolss, G.W., Jung, M., 1978. Travelling Atmospheric disturbances as a possible explanation for daytime positive storm effects of moderate duration at middle latitudes. J. Atmos. Terr. Phys. 40, 1351–1354.
Prolss, G.W., 1980. Magnetic storm associated perturbation of the upper atmosphere: recent results obtained by satellite-borne analyzers. Rev. Geophys. Space Phys. 18, 183–202.
Prolss, G.W., 1993. Common origin of positive ionospheric storms at middle latitudes and the geomagnetic activity effect at low latitudes. J. Geophys. Res. 98 (A4), 5981–5991.
Prolss, G.W., 1995. Ionospheric F-region storms. In: Volland, H. (Ed.), in Handbook of Atmospheric Electrodynamics. CRC Press, Boca Raton, Fla.
Prolss, G.W., 1997. Magnetic storm associated perturbations of the upper atmosphere. In: Tsurutani, B.T., et al. (Eds.), Magnetic Storms, Geophys. Monogr. Ser vol. 98. AGU, Washington, DC, pp. 227–241.
Reddy, C.A., Mayr, H.G., 1998. Storm-time penetration to low latitudes of magnetosphericionospheric convection and convection-driven thermospheric winds. Geophys. Res. Lett. 25, 3075–3078.
Richards, P.G., Wilkinson, P.J., 1998. The ionosphere and thermosphere at southern midlatitudes during the November 1993 ionospheric storm: a comparison of measurement and modeling. J. Geophys. Res. 103, 9373.
Sahai, Y., Aarons, J., Mendillo, M., Baumgardner, J., Bittencourt, J.A., Takahashi, H., 1994. OI 630 nm imaging observations of equatorial plasma depletions at 16 °S dip latitude. J. Atmos. Terr. Phys. 56, 1461–1475.
Sahai, Y., Fagundes, P.R., Bittencourt, J.A., 2000. Transequatorial F-region ionospheric plasma bubbles: solar cycle effects. J. Atmos. Terr. Phys. 62, 1377–1383.
Sahai, Y., Fagundes, P.R., Becker-Guedes, F., Bolzan, M.J.A., Abalde, J.R., Pillat, V.G., de Jesus, R., Lima, W.L.C., Crowley, G., Shiokawa, K., MacDougall, J.W., Lan, H.T., Igarashi, K., Bittencourt, J.A., 2005. Effects of the major geomagnetic storms of October 2003 on the equatorial and low-latitude F region in two longitudinal sectors. J. Geophys. Res. 110, A12S91. http://dx.doi.org/10.1029/2004JA010999.
Sahai, Y., Becker-Guedes, F., Fagundes, P.R., de Jesus, R., de Abreu, A.J., Paxton, L.J., Goncharenko, L.P., Brunini, C., Gende, M., Ferreira, A.S., Lima, N.S., Guarnieri, F.L., Pillat, V.G., Bittencourt, J.A., Candido, C.M.N., 2009a. Effects observed in the Latin American sector ionospheric F region during the intense geomagnetic disturbances in the early part of November 2004. J. Geophys. Res. 114, A00A19. http://dx.doi.org/10.1029/2007JA013007.
Sahai, Y., Becker-Guedes, F., Fagundes, P.R., de Abreu, A.J., de Jesus, R., Pillat, V.G., Abalde, J.R., Martinis, C.R., Brunini, C., Gende, M., Huang, C.-S., Pi, X., Lima, W.L. C., Bittencourt, J.A., Otsuka, Y., 2009b. Observations of the F-region ionospheric irregularities in the South American sector during the October 2003 "Halloween Storms". Ann. Geophys. 27, 4463–4477. http://dx.doi.org/10.5194/angeo-27-4463-2009.
Sahai, Y., Becker-Guedes, F., Fagundes, P.R., de Jesus, R., de Abreu, A.J., Otsuka, Y., Shiokawa, K., Igarashi, K., Yumoto, K., Huang, C.-S., Lan, H.T., Saito, A., Guarnieri, F.L., Pillat, V.G., Bittencourt, J.A., 2009c. Effects observed in the ionospheric F region in the east Asian sector during the intense geomagnetic disturbances in the early part of November 2004. J. Geophys. Res. 114, A00A18. http://dx.doi.org/10.1029/2008JA013053.
Sahai, Y., Fagundes, P.R., de Jesus, R., de Abreu, A.J., Crowley, G., Kikuchi, T., Huang, C.-S., Pillat, V.G., Guarnieri, F.L., Abalde, J.R., Bittencourt, J.A., 2011. Studies of ionospheric F-region response in the Latin American sector during the geomagnetic storm of 21–22 January 2005. Ann. Geophys. 29, 919–929. http://dx.doi.org/10.5194/angeo-29-1-2011.
Schunk, R.W., Nagy, A.F., 2000. Ionospheres: Physics Plasma Physics and Chemistry. Cambridge University Press, USA.
Schunk, R.W., Sojka, J.J., 1996. Ionosphere–thermosphere space weather issues. J. Atmos. Terr. Phys. 58, 1527–1574.
Sobral, J.H.A., Abdu, M.A., Gonzalez, W.D., Tsurutani, B.T., Batista, I.S., Gonzalez, A.L. C., 1997. Effects of intense storms and substorms on the equatorial ionosphere/thermosphere system in the American sector from ground-based and satellite data. J. Geophys. Res. 102, 14305–14313.
Sobral, J.H.A., Abdu, M.A., Yamashita, C.S., Gonzalez, W.D., Gonzalez, A.C., Batista, I. S., Zamlutti, C.J., Tsuruatni, B.T., 2001. Responses of the low-latitude ionosphere to very intense geomagnetic storms. J. Atmos. Terr. Phys. 63, 965–974.
Sultan, P.J., 1996. Linear theory and modeling of the Rayleigh–Taylor instability leading to the ocurrence of equatorial spread-F. J. Geophys. Res. 101 (A12), 26875–26891.
Tiwari, R., Strangeways, H.J., Tiwari, S., Ahmed, A., 2013. Investigation of ionospheric irregularities and scintillation using TEC at high latitude. Adv. Space Res. 52, 1111–1124.
Tsurutani, B.T., Gonzalez, W.D., 1997. The Interplanetary causes of magnetic storms: A review. In: Tsurutani, B.T., et al. (Eds.), Magnetic Storms, Geophys. Monogr. Ser vol. 98. AGU, Washington, D. C, pp. 77–89. http://dx.doi.org/10.1029/GM098p0077.
Wanninger, L., 1993. Effects of the equatorial ionosphere on GPS. GPS World, 48–54.
Warnant, R., Pottiaux, E., 2000. The increase of the ionospheric activity as measured by GPS. Earth Planets Space 52, 1055–1060.
Whalen, J.A., 2002. Dependence of equatorial bubbles and bottomside spread-F on season, magnetic season, and E x B drift velocity during solar maximum n. A2 (SIA 3-1). J. Geophys. Res. 107, 3–9.
Yeh, H.C., Foster, J.C., Rich, F.J., Swider, W., 1991. Storm time electric field penetration observed at midlatitude. J. Geophys. Res. 96, 5707.
Yeh, K.C., Liu, C.H., 1982. Radio wave scintillations in the ionosphere. Proced. IEEE 70, 324–360.